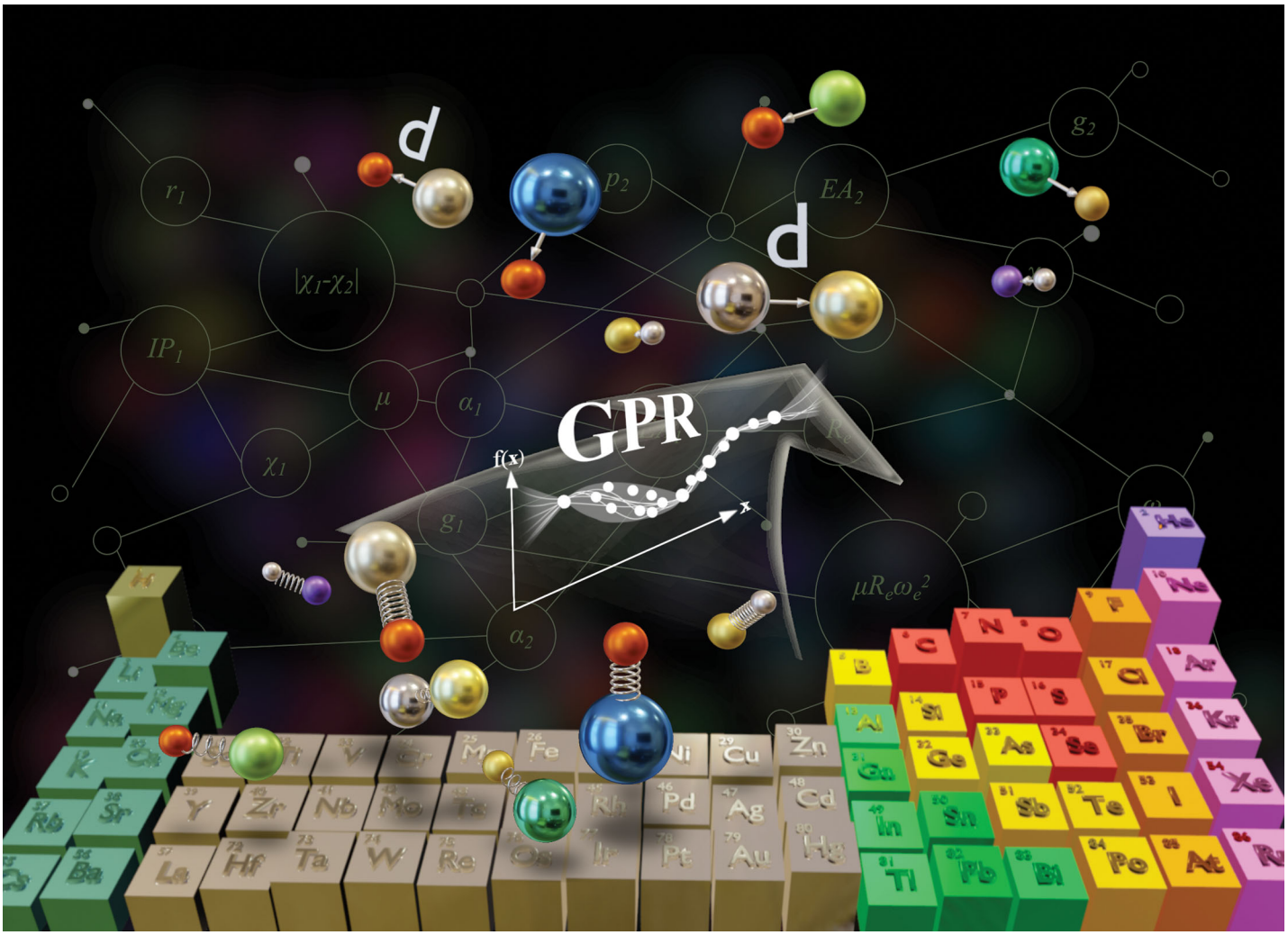

Showcasing research from the group of Dr Jesús Pérez Ríos, Fritz-Haber-Institut der Max-Planck-Gesellschaft.

A data-driven approach to determine dipole moments of diatomic molecules

The Pérez Ríos group works at the border between data-driven science and theoretical atomic, molecular, and optical physics, bringing a new perspective to the realm of atoms and molecules. As an example, in this work, it is shown that Gaussian process regression (GPR) can accurately predict dipole moments of diatomic molecules once appropriate atomic and molecular features are employed. The features involve a combination of molecular properties that help to improve our knowledge of the ultimate nature of dipole moments.

As featured in:

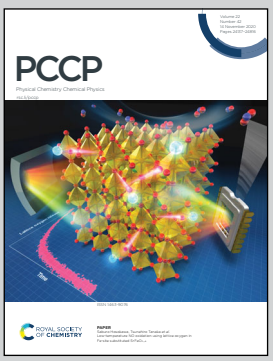

See Jesús Pérez-Ríos *et al.*, *Phys. Chem. Chem. Phys.*, 2020, **22**, 24191.

ROYAL SOCIETY OF CHEMISTRY

rsc.li/pccp

Registered charity number: 207890

PCCP

PAPER

View Article Online
View Journal | View Issue

Cite this: *Phys. Chem. Chem. Phys.*, 2020, **22**, 24191

A data-driven approach to determine dipole moments of diatomic molecules

Xiangyue Liu, Gerard Meijer and Jesús Pérez-Ríos *

Received 17th July 2020,
Accepted 22nd August 2020

DOI: 10.1039/d0cp03810e

rsc.li/pccp

We present a data-driven approach for the prediction of the electric dipole moment of diatomic molecules, which is one of the most relevant molecular properties. In particular, we apply Gaussian process regression to a novel dataset to show that dipole moments of diatomic molecules can be learned, and hence predicted, with a relative error $\lesssim$5%. The dataset contains the dipole moment of 162 diatomic molecules, the most exhaustive and unbiased dataset of dipole moments up to date. Our findings show that the dipole moment of diatomic molecules depends on atomic properties of the constituents atoms: electron affinity and ionization potential, as well as on (a feature related to) the first derivative of the electronic kinetic energy at the equilibrium distance.

1 Introduction

The study of relationships between spectroscopic constants is a traditional topic in chemical physics since the pioneering work of Kratzer and Mecke, among others[1–6] and is beautifully summarized by Varshini.[7,8] Recently, we have shown that some spectroscopic constants are universally related,[9] *i.e.*, the relationships between them are independent of the nature of the molecular bond. However, the electric dipole moment of a molecule, despite being an essential molecular property, has not been considered in previous studies about relationships between spectroscopic constants. Only recently, there have been some efforts towards the understanding of the dipole moment in terms of molecular spectroscopic constants. As a result, it has been found by Hou and Bernath that the expression for the dipole moment, d, taught in elementary chemistry courses

$$d = qR_e, \tag{1}$$

where q is the effective charge and R_e denotes the equilibrium bond length of the molecule, does not capture the proper physics of the dipole moment in many molecules.[10,11] They also demonstrated that the dipole moment of some molecules can be predicted from the effective charge (obtained from quantum chemistry calculations) and spectroscopic constants of molecules.

In the 2000s the big data-driven science paradigm emerged in the scientific community.[12] In this new paradigm, machine learning techniques are among the most prominent tools to assess scientific knowledge. To be precise, adequately formatted data are used to identify unexpected correlations and to predict observables based on patterns and trends of the data. When applied to physics, this novel paradigm lets nature speak up through hidden and intriguing correlations that lead to the formulation of new questions beyond a specific physical model. In particular, in chemical physics, as recently shown, data-driven approaches bring a new perspective to solve some of the most delicate problems of the field.[13–16]

In this paper, we present a data-driven approach to dipole moments of diatomic molecules and its relationship with spectroscopic constants. We show that, after compiling the most exhaustive list of dipole moments for diatomics up to date (to the best of our knowledge) into a dataset, it is possible to learn the dipole moment of diatomic molecules based upon atomic and molecular properties with a relative error $\lesssim$5%. The number of molecules in our dataset, classified by the type of the constituent atoms, is given in Fig. 1. Our results reveal that it is not possible to predict the dipole moment of a molecule solely from atomic properties, although this is feasible for the spectroscopic constants,[9] but that it is necessary to include molecular features. The molecular spectroscopic constants are needed in a combination that describes the force on the electrons at the equilibrium distance, *i.e.*, in a combination that has the same functional dependence as the first derivative of the electronic kinetic energy at the equilibrium distance.

2 An overview on the nature of the electric dipole moment of molecules

The study of the nature of the electric dipole moment of molecules is a traditional topic in quantum chemistry that has fascinated the chemical physics community for almost a century by now. The first explanation of the nature of the electric dipole moment of

Fritz-Haber-Institut der Max-Planck-Gesellschaft, Faradayweg 4-6, 14195 Berlin, Germany. E-mail: jperezri@fhi-berlin.mpg.de

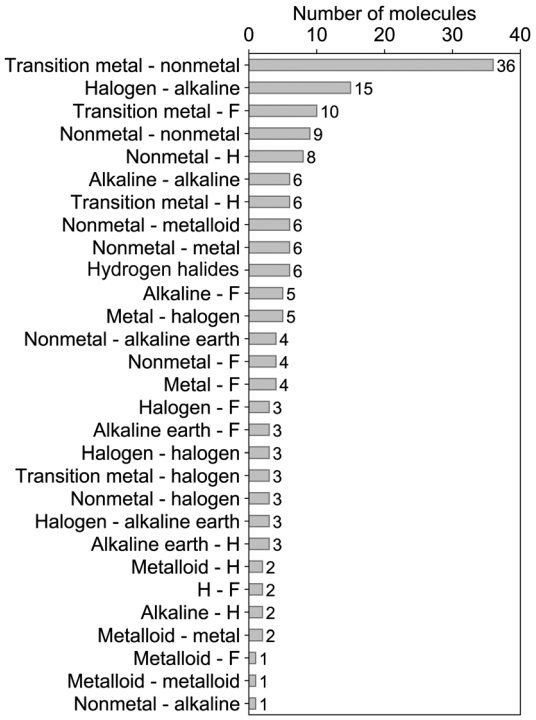

Fig. 1 Molecules in the whole dataset classified by the types of their constituent atoms.

molecules is due to Pauling in the 1930s.[17] In particular, after studying hydrogen halide molecules, Pauling proposed that the dipole moment of a molecule is correlated with the relevance of the ionic structure with respect to the covalent one at the equilibrium bond length of the molecule. In this model, the dipole moment is a consequence of the charge transfer between the atoms within the molecule. Therefore, the larger the charge transfer, the bigger the dipole moment is. The charge transfer is quantized by the ionic character (IC), which is given by

$$\mathrm{IC} = \frac{d}{eR_e}, \tag{2}$$

where e is the electron charge. Comparing eqn (2) and (1), it is clear that the ionic character is equivalent to the effective charge, q, placed at the center of each of the atoms forming the molecule, as prescribed by eqn (1). However, Pauling's model does not predict 100% of ionic character for molecules that are fully ionic, like the alkali metal halides. Despite the slight inaccuracy of Pauling's model in predicting dipole moments, it is worth emphasizing that Pauling realized that the dipole moment of a molecule must be related to other molecular properties through the molecular bond.

The next step towards understanding the electric dipole moment was the introduction of a new concept: the homopolar dipole moment, d_h, by Mulliken. In particular, Mulliken realized that because the atomic orbitals are different in size, the overlap between those leads to a charge displacement with respect to the midpoint of the equilibrium bond length, which affects the electric dipole moment of the molecule.[18] Furthermore, Mulliken noticed that the asymmetry in the charge distribution of hybrid orbitals causes the so-called atomic dipole moment, d_a. The models of Mulliken and Pauling were summarized and further developed by Coulson,[19] who proposed the ultimate expression for the dipole moment of a diatomic molecule as

$$d = eR_e + d_a + d_h + d_p, \tag{3}$$

where d_p is the contribution due to the polarization of the atomic orbitals to the dipole moment of the molecule. One has to realise that eqn (3), although being more precise than eqn (1), requires the input from quantum chemistry calculations. For a summary on the Pauling and Mulliken models, we recommend the comprehensive review of Klessinger.[20]

The models of Pauling and Mulliken have been accepted by the physical chemistry community and taught in elementary chemistry courses for a long time, despite the fact that neither one of those is fully satisfactory. Recently, Hou and Bernath,[10,11] after studying the experimentally determined dipole moments of an extensive group of molecules and using quantum chemistry calculations, have suggested that the electric dipole moment of a molecule should be given as

$$d = qR_d \tag{4}$$

where q is the effective charge and R_d is an effective length that depends on fundamental spectroscopic constants of the molecule with $R_d < R_e$. Both eqn (3) and (4) rely on the input of quantum chemistry calculations, in particular on the results from a natural bond orbital analysis. Therefore, the electric dipole moment of diatomic molecules still lacks a satisfactory and accurate explanation in terms of fundamental spectroscopic constants.

3 Machine learning model

3.1 Gaussian process regression

Finding relationships of the dipole moment with spectroscopic constants can be viewed as a regression problem, where the goal is to learn the mapping from the input atomic and molecular features $\mathbf{x}$ onto the target property, y, which in this case is the electric dipole moment, by a function $y = f(\mathbf{x})$. In the present work, we use Gaussian process regression (GPR) to approximate the function $f(\mathbf{x})$. As a non-parametric probabilistic method, GPR does not presume a functional form of $f(\mathbf{x})$ before observing the data. Instead, it infers a Gaussian distribution of functions over function space by a Gaussian process[21,22]

$$f(\mathbf{x}) \sim \mathrm{GP}(m(\mathbf{x}), k(\mathbf{x},\mathbf{x}')), \tag{5}$$

determined by a mean function, $m(\mathbf{x})$, and a kernel (covariance) function, $k(\mathbf{x},\mathbf{x}')$. The prior, $p(f|\mathbf{x})$, spanning in the function space, after exposed to the observations, is constrained into a posterior, $p(f|\mathbf{x},y)$, based on the Bayes theorem. The predictions, y^*, can then be made for new input atomic and molecular features, $\mathbf{x}$, through the posterior.

The kernel function, $k(\mathbf{x},\mathbf{x}')$, captures the smoothness of the response and intrinsically encodes the behaviour of the model acting on the input. The kernel functions can be chosen

by presuming the behaviour of the response to the input feature by observing the data. Its functional form and the possible hyperparameters can also be determined by a cross-validation (CV).[23]

3.2 Model evaluation

In learning the dipole moments, the dataset is divided into training and test sets. As a data-driven approach, GPR learns the relationship between the input features and dipole moments by observing the training set, while the predictive performance of the GPR models is examined with the test set. In this work, 20 molecules are used in the test set, while the rest are used in the training set. For the training/test splitting, the dataset is first stratified into 20 strata based on the dipole moments' true values. A Monte Carlo (MC) approach is then performed to select the 20 test data from the dataset randomly. In each MC step, a GPR model is trained based on the training set with 5-fold cross-validation. The generalization performance of the model is then evaluated with the test set. In the end, the mean and standard deviation (STD) of the test-set errors are reported in this work, obtained from 1000 MC training/test splittings. Details about this MC approach will be discussed elsewhere.[24]

The performance evaluation of the GPR models is carried out through three different estimators:

• The mean absolute error (MAE) defined as

$$\mathrm{MAE} = \frac{1}{N}\sum_{i=1}^{N}|y_i - y_i^*|, \tag{6}$$

where y_i are the true values of dipole moments, y_i* are the predictions, and N is the number of observations in the dataset.

• The root mean square error (RMSE), which reads as

$$\mathrm{RMSE} = \sqrt{\frac{1}{N}\sum_{i=1}^{N}(y_i - y_i^*)^2}. \tag{7}$$

• The normalized error, r_E, defined as the ratio of the RMSE to the range of the data

$$r_E = \frac{\mathrm{RMSE}}{y_{max} - y_{min}}. \tag{8}$$

4 The dataset

The dataset employed in this work consists of ground-state dipole moments of 162 polar diatomic molecules, 139 of which have both information on the equilibrium bond length, R_e, and the harmonic vibrational frequency, ω_e. The dataset is presented in Table 4 of the Appendix and it constitutes the most extensive dataset for dipole moments of diatomic molecules that we are aware of. Nevertheless, for more efficient scrutiny of our dataset's generality, we show in Fig. 2 the equilibrium bond length, R_e, *versus* the electric dipole moment of diatomic molecules. The density plots and the box plots show the distribution of R_e (right) and dipole moment, d, (top), respectively.

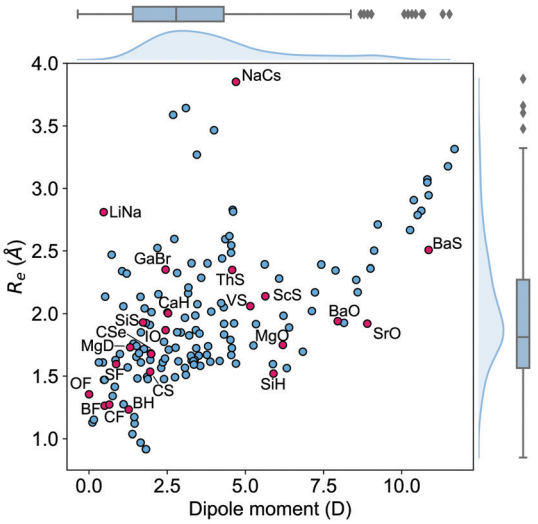

Fig. 2 The equilibrium bond length R_e *versus* the electric dipole moment of the molecules in the dataset. The blue filled circles are the molecules that can be learned by the GPR model in this work. The red filled circles indicate the molecules that can hardly be described by the GPR model in this work. These molecules are labeled by their chemical formula. The density in the right part and upper part of the figure shows the kernel density distribution of R_e and dipole moments, respectively. The box plot shows the minimum, the maximum, the sample median, and the first and third quarterlies of R_e (right) and dipole moments (top).

The equilibrium bond length of the molecules is distributed between 0.9 and 3.9 Å with a median of around 1.5 Å, although most of the molecules show an equilibrium bond length between 1.2 and 3.2 Å. The dipole moment values in the dataset range from 0.0043 D to 11.69 D with a median of around 2.45 D, which shows the large variety of molecules included in the dataset.

The dataset can also be categorized in terms of the type of atoms constituting the molecules, as it is shown in Fig. 1. In this figure, it is noticed that most of the molecules in the dataset present a highly ionic bond resulting from a transition metal and a nonmetal atom. The second most prominent group of molecules contains a halogen atom and an alkaline atom, which shows an ionic bond. The rest of the molecules exhibit a bond from partially ionic to highly ionic, which shows the diversity of the dataset.

5 Results and discussion

We have used a GPR approach to learn the diatomic molecules' dipole moment employing features coming from different atomic and molecular properties. The atomic properties considered are the electron affinity (EA) taken from ref. 25–27, ionic potential (IP) taken from ref. 28, electronegativity (χ) and polarizability (α) taken from ref. 25, whereas the molecular properties are the reduced mass, μ, equilibrium bond length, R_e, and the harmonic vibrational frequency, ω_e. The atomic properties employed are related to the intrinsic chemical nature of the dipole moment due to the polarity of a molecular orbital

Table 1 GPR Predictions on the ground-state dipole moments. g_i, p_i, EA_i, IP_i, χ_i, α_i are groups, periods, electron affinity, ionic potential, electronegativity and polarizability of the atom i, respectively. μ is the reduced mass of a molecule. For these results we employ 118 from the dataset out of the 139 molecules having values for both R_e and ω_e

Feature	Test RMSE (D)	Test MAE (D)	Test r_E (%)
$(EA_1, EA_2, IP_1, IP_2, \sqrt{\mu R_e \omega_e^2})$	0.56 ± 0.02	0.43 ± 0.0004	4.8 ± 0.1
$(\chi_1, \chi_2, \sqrt{\mu R_e \omega_e^2})$	0.70 ± 0.05	0.52 ± 0.03	6.0 ± 0.4
$(EA_1, EA_2, IP_1, IP_2, \chi_1, \chi_2)$	0.86 ± 0.006	0.65 ± 0.02	7.4 ± 0.05
(EA_1, EA_2, IP_1, IP_2)	0.97 ± 0.05	0.74 ± 0.05	8.3 ± 0.4
$(EA_1, EA_2, IP_1, IP_2, R_e)$	1.04 ± 0.02	0.81 ± 0.04	9.1 ± 0.2
$(\chi_1, \chi_2, \alpha_1, \alpha_2)$	1.29 ± 0.004	1.01 ± 0.007	11.2 ± 0.04
(χ_1, χ_2)	1.35 ± 0.002	1.05 ± 0.009	11.7 ± 0.01
$(\sqrt{\lvert\chi_1 - \chi_2\rvert}, \bar{\alpha}, {D_0}^{-1})$	1.21 ± 0.03	0.96 ± 0.03	10.5 ± 0.3
$(p_1, p_2, g_1, g_2, R_e)$	1.25 ± 0.02	0.94 ± 0.04	10.8 ± 0.1

in the molecular-orbital bond theory or to the ionic character of the molecular bond within the valence-bond theory.[19] The GPR performance for different features is summarized in Table 1, where we employ 118 out of the 139 molecules from the dataset having values for both R_e and ω_e. The permutational invariance of the GPR models upon exchanging the two elements in a molecule (*e.g.*, from molecule AB to BA) is ensured by permutation of the training sets.

After using different combinations of atomic and molecular properties, we find that the dipole moment of a diatomic molecule can be best learned by a GPR model using (EA_1, EA_2, IP_1, IP_2, $\sqrt{\mu R_e \omega_e^2}$) as the input features. The performance of this model is shown in Fig. 3. The predicted values reproduce the true values very well with a small deviation that leads to a normalized error $r_E < 5\%$ (RMSE = 0.56 ± 0.02 D). We have also computed the learning curve of the cited GPR model, which gives an intuitive idea about the model's learning and generalization performance concerning the size of the training set. The results are shown in the inset of Fig. 3. The training RMSE and test RMSE are shown as a function of the number of training data points $N_{Training}$. The learning curve's shade shows the variance of training/test RMSE, obtained for each point from a MC approach of 500 training/test splittings. The mean test error decreases with increasing training data. In particular, with 80 training data, the learning curve is almost converged, suggesting that this model can not benefit from more data of the same dataset. The error's variance shows the ability of the model to be employed in different subgroups of molecules. In this case, the variance of test RMSE becomes smaller as the number of training data increases and converges to <0.02 D with 60 training data.

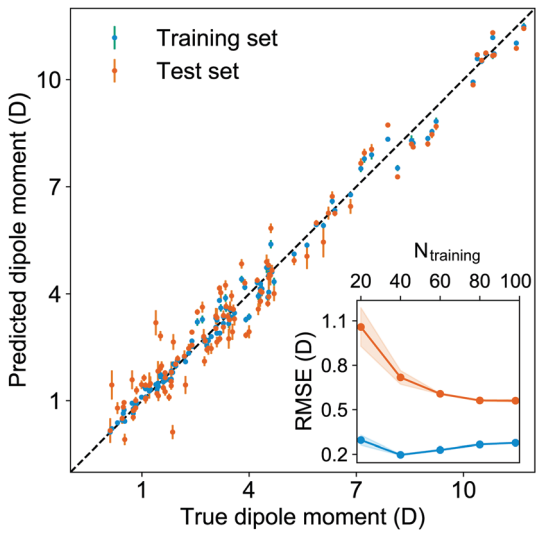

Fig. 3 The GPR predictions of the ground-state dipole moments. The values shown in this figure are the average of predictions from 1000 MC sampled training/test splittings.[24] The test set contains 20 molecules, while the training set contains 98 molecules. The mean and standard derivation of the predictions are shown for each molecule when they are used as training data (shown in blue) and test data (shown in orange). The inset shows the learning curve, which shows the training and test RMSE of the model with respect to the number of training data $N_{training}$. The shade in the learning curve shows the variance of training/test RMSE, obtained for each point from a MC approach of 500 training/test splittings.

In previous work, we have shown that R_e, ω_e, and the binding energy of a diatomic molecule can be learned through groups and periods of the constituent atoms as features.[9] However, the same features dramatically fail in learning the dipole moment. In particular, we find that the test errors are RMSE = 1.25 ± 0.02 D and r_E = 10.8 ± 0.1%, respectively. In our view, this is an indication of the more intricate nature of the dipole moment compared to the spectroscopic constants of diatomic molecules.

In ref. 29 it is shown that the dipole moment of diatomic alkali–alkaline earth molecules can be empirically calculated from the difference in the electronegativity of the constituent atoms $\sqrt{\lvert\chi_1 - \chi_2\rvert}$, the mean atomic polarizabilities $\bar{\alpha} = (\alpha_1 + \alpha_2)/2$ and the dissociation energy D_e. We have generalized this idea trough a GPR model by using ($\sqrt{\lvert\chi_1 - \chi_2\rvert}$, $\bar{\alpha}$, ${D_0}^{-1}$) as features and applied it to the present dataset, despite the fact that alkaline earth–alkaline molecules are absent in the dataset. We have used the binding energy, D_0, instead of the dissociation energy, as the former is tabulated more frequently. As a result, we find a normalized error r_E = 10.5 ± 0.3%, which indicates that some of the physics behind the dipole moment function of alkali–alkaline earth molecules is applicable to any other molecule. This is an unexpected result that shows the underlying universality of the physics of the dipole moment.

The outstanding performance of (EA_1, EA_2, IP_1, IP_2, $\sqrt{\mu R_e \omega_e^2}$) as features implies that the accepted picture in chemistry in which the difference of the electronegativity of the atoms within a molecule establishes the ionic character of the molecular bond[17,19,30] is not sufficient to characterize the dipole moment of a molecule. When using the electron affinity and the atoms' ionization potential as features, the performance improves by 25%. However, only if $\sqrt{\mu R_e \omega_e^2}$ is included as a feature, the dipole moment is predicted with a RMSE below 0.7 D. Therefore, we find that it is essential to add $\sqrt{\mu R_e \omega_e^2}$ as a feature in describing the dipole moment of a diatomic molecule. It can be shown that this feature is related to the

derivative of the electronic kinetic energy, $T(R)$, at the equilibrium bond length as[31]

$$-\left.\frac{\mathrm{d}T(R)}{\mathrm{d}R}\right|_{R=R_e} = \mu R_e \omega_e^2, \tag{9}$$

which represents a force within the molecule. When equating this force to the pure electrostatic force, one obtains R_d and, through eqn (4), it is then possible to define the ionic character as

$$\mathrm{IC} = 100\left(d\sqrt{\mu R_e \omega_e^2}\right)^{1/2}, \tag{10}$$

where the value of IC is given in percent. It is seen that IC does not directly depend upon the electronegativity differences of the atoms, contrary to the accepted picture in chemistry. The feature $\sqrt{\mu R_e \omega_e^2}$ was first introduced by Hou and Bernath[10,11] as an empirical relationship, and we use this here to define the ionic character of a molecular bond.

Alternatively, the ionic character can be defined in terms of the electronegativity difference between the two atoms forming a molecule as

$$\mathrm{IC} = 16|\chi_1 - \chi_2| + 3.5|\chi_1 - \chi_2|^2, \tag{11}$$

following Hannay and Smyth.[30] Surprisingly, eqn (10) and (11) lead to different results for the ionic character of the molecules in the database, as shown in Fig. 4, where it is noticed that the distribution of the ionic character following eqn (11) appears to the complement to the one obtained from eqn (10). This is related to the fact that the model of Hou and Bernath (eqn (10)) systematically leads to a larger ionic character than the model of Hannay an Smyth.

The GPR model with (EA_1, EA_2, IP_1, IP_2, $\sqrt{\mu R_e \omega_e^2}$) as input features shows several outliers. To see the importance of these outliers we have compared the distribution of the ionic character and dipole moment of the molecules in Fig. 4 (shown in grey) with the same magnitudes for the subset of 118 molecules that can be learned in this work (shown in blue). The ML-learned subset has similar overall distributions of dipole moments and ionic characters in comparison with the whole dataset. Therefore the outliers do not significantly modify the underlying distribution that the molecules follow.

In Table 2, it is shown a classification of the outliers as a function of its molecular bond and constituent atoms. The effective atomic charges of these molecules are also calculated with a density functional theory (DFT) approach, which is shown in Table 3 utilizing different charge partitioning methods. The calculations are performed with the B3LYP functional[32] and def2-TZVP basis set,[33–35] with the Gaussian 16 package.[36] We have noticed that for these outliers, the natural bond orbital (NBO) method gives larger effective atomic charges compares to the Mulliken population. Furthermore, all the molecules showing a NBO charge larger than 1.0 are the ones showing an ionic character in virtue of eqn (10) above 100%. For the outliers within the van der Waals molecules, we find LiNa and NaCs. LiNa has the smallest R_e and dipole moment of the bialkaline molecules in this dataset, while NaCs has the largest R_e and dipole moment.

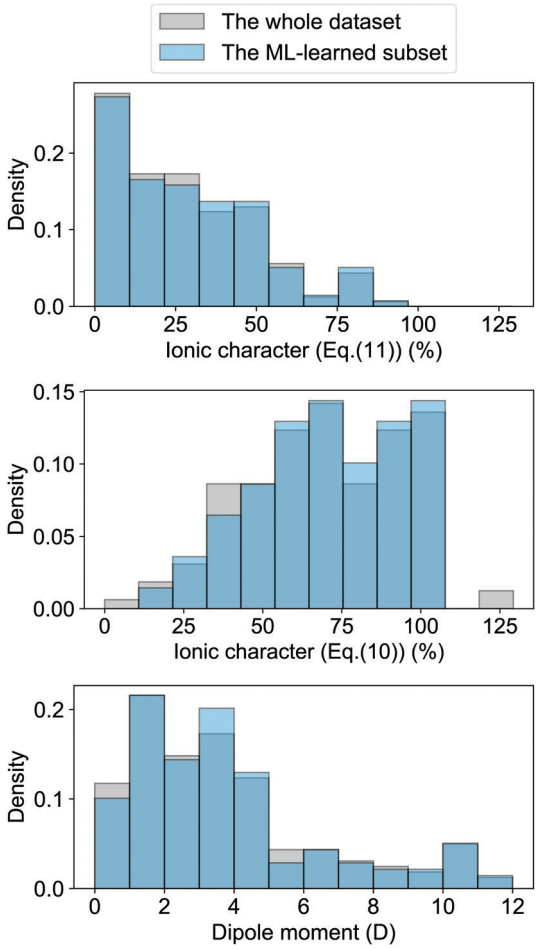

Fig. 4 Comparison of the histograms of ionic characters and dipole moments in the whole dataset (shown in grey) and the ML-learned subset of 118 molecules (shown in blue). Panel (a) and (b) show the ionic characters calculated from eqn (10) and (11), respectively. Panel (c) plots the histogram of the dipole moment of the molecules. It is worth noticing that the dark blue regions appear in regions where the grey and light-blue bars overlap.

Table 2 Outliers for learning the electric dipole moment of diatomic molecules. These molecules are labeled in Fig. 2 and classified with the types of constituent atoms and the molecular bonds

Type of bond	Molecule
Nonmetal–nonmetal	IO, CS, SiS, CSe
Nonmetal–F	SF, BF, CF, OF
Metal–halogen	GaBr
Alkaline earth–nonmetal	BaO, SrO, MgO, SrS, BaS
Alkaline earth–H	MgD, CaH
Metalloid–H	BH, SiH
Transition metal–nonmetal	VS, ScS, ThS
van der Waals	LiNa, NaCs

To understand the effect of different bonding types on the dipole moment, we plot in Fig. 5 the relationships between R_e and dipole moments for different kinds of molecules in the current dataset, where the outliers are shown in red circles. We observe that the relationships between R_e and dipole moments depend on the type of molecule under consideration. As shown in

Table 3 The effective atomic charges of the outliers with different charge partitioning methods, calculated with the B3LYP functional[32] and def2-TZVP basis set[33–35] with the Gaussian 16 package[36]

Molecule	Mulliken	Hirshfeld	NBO
MgO	0.694	0.576	1.278
SrO	0.871	0.714	1.496
BaO	0.838	0.640	1.508
BaS	0.759	0.660	1.437
BF	0.099	0.073	0.549
CF	0.030	0.014	0.315
OF	0.017	0.012	0.063
SF	0.198	0.108	0.431
MgD	0.187	0.241	0.657
CaH	0.276	0.318	0.738
BH	−0.036	0.072	0.349
SiH	0.048	0.122	0.349
SiS	0.231	0.222	0.656
CS	−0.081	−0.087	−0.174
SeC	0.180	0.104	0.263
IO	0.412	0.214	0.625
GaBr	0.331	0.265	0.627
ScS	0.529	0.452	0.743
VS	0.425	0.247	0.343
CsNa	0.140	0.161	0.279
NaLi	−0.074	0.001	0.007

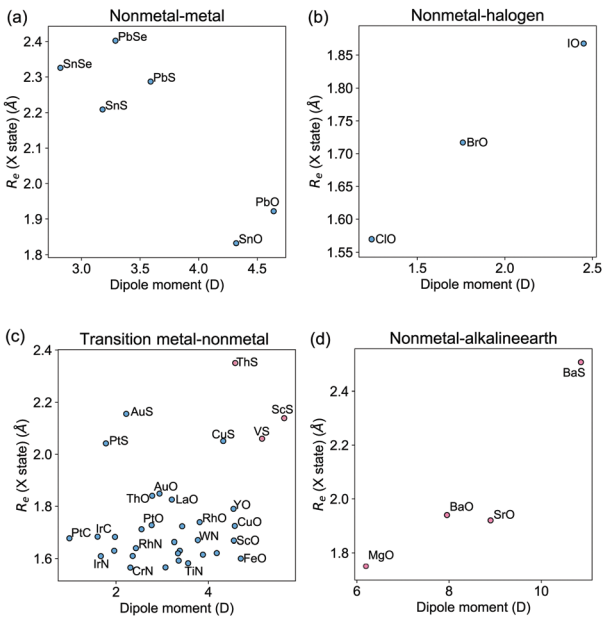

Fig. 5 The equilibrium bond lengths R_e as a function of dipole moments, classified by the type of the constituent atoms. The molecules that can be described by the GPR models from (EA_1, EA_2, IP_1, IP_2, $\sqrt{\mu R_e \omega_e^2}$) are shown in blue circles, while the outliers are shown in red circles.

panel (a) of Fig. 5, R_e and dipole moments show linear relationship for metal–nonmetal molecules, in which the nonmetals atoms are from the same group in the periodic table. Similarly, linear behaviors have also been observed for the group IV/VI diatomic molecules in ref. 37. For the oxygen halides shown in panel (b), R_e increases almost linearly with the dipole moment. In panel (c), the molecules containing a transition metal and a nonmetal atom show a different trend of the equilibrium distance as a function of the dipole moment compared with the molecules formed by the main-group metal elements nonmetal atoms in panel (a). Within these molecules, the outliers are the ones with both the largest dipole moments and R_e in panel (c). Interestingly, we find that all the 4 alkaline earth–nonmetal molecules in the dataset are outliers, as shown in panel (d) of Fig. 5, which correlate with an NBO population larger than 1, as shown in Table 3. In particular SrO, BaO and BaS have the largest atomic charges within the molecules in the dataset.

6 Conclusions

In summary, we have shown that through a GPR model, the ground state dipole moments of diatomic molecules can be related to spectroscopic constants, namely R_e and ω_e. More specifically, without any quantum chemistry calculation, the dipole moments of molecules have been predicted with an error $\lesssim 5\%$ by using both atomic features, including electron affinity, and ionic potential, and a combination of molecular spectroscopic constants, $\sqrt{\mu R_e \omega_e^2}$. In addition, we find that the difference in the electronegativity of the constituents atoms is not sufficient to describe the dipole moments of the diatomic molecules in stark contrast with what is generally assumed in general chemistry. Therefore, our data-driven approach shows that the nature of the dipole moment is more intricate than for spectroscopic constants, and it is clearly correlated with the very fundamental nature of the chemical bond. Finally, it is worth emphasizing that our findings have been possible thanks to the development of a complete and unbiased dataset.

Conflicts of interest

There are no conflicts to declare.

Appendix 1. Details about GPR

The kernel function employed in this work, which gives the best CV scores, is the rational quadratic kernel[22] defined by

$$k(x_i, x_j|\theta) = \sigma_l^2 \left(1 + \frac{r^2}{2\alpha\sigma_l^2}\right)^{-a}, \quad (12)$$

where σ_l is the length scale, α is a scale-mixture parameter and r is the Euclidean distance between x_i and x_j defined as

$$r = \sqrt{(x_i - x_j)^{\mathrm{T}}(x_i - x_j)}. \quad (13)$$

Appendix 2. The dataset for dipole moment of diatomic molecules

The dataset is summarized in Table 4, which consists of dipole moments, d, of 162 polar diatmonic molecules, 156 of which have information about equilibrium bond length, R_e, while 139 also have harmonic vibrational frequency, ω_e. The references of the dipole moments are also listed in the table.

Table 4 The dipole moments, d, equilibrium bond length, R_e, and harmonic vibrational frequency, ω_e, employed in this work. The references to the dipole moments are also listed in the table. R_e and ω_e are taken from ref. 38 and 39, or the same reference of the dipole moment of the corresponding molecules, except as indicated

Molecule	d (D)	R_e (Å)	ω_e (cm^{-1})	Ref.	Molecule	d (D)	R_e (Å)	ω_e (cm^{-1})	Ref.	Molecule	d (D)	R_e (Å)	ω_e (cm^{-1})	Ref.
AgBr	5.62	2.393	247.7	25	GeTe	1.06	2.34	323.9	40	PbSe	3.29	2.402	277.6	40
AgCl	6.08	2.281	343.5	25	DBr	0.823	1.415	1884.8	41	PbTe	2.73	2.595	212	40
AgF	6.22	1.983	513.5	42	HBr	0.8272	1.414	2649	25	PN	2.7514	1.491	1337.2	43
AgH	2.86	1.618	1759.9	44	DF	1.819	0.917	2998.2	41	PO	1.88	1.476	1233.3	45
AgI	4.55	2.545	206.5	25	HF	1.826526	0.917	4138.3	46	PtC	0.99	1.677	1051.1	47
AlF	1.515	1.654	802.3	48	HfF	1.66	1.85		49	PtF	3.42	1.868		50
AuF	4.32	1.918	539.4[a]	51	HfO	3.431	1.723	974.1	52	PtN	1.977	1.682		53
AuO	2.94	1.849	624.59[b]	54	HI	0.448	1.609	2309	25	PtO	2.77	1.727	851.1	47
AuS	2.22	2.156	410.19[c]	54	IBr	0.726	2.469	268.6	25	PtS	1.78	2.042		47
BaF	3.17	2.163	468.9	55	ICl	1.207	2.321	384.3	56	RbBr	10.86	2.945	169.5	57
BaO	7.955	1.94	669.8	58	ID	0.316	1.609	1639.7	59	RbCl	10.51	2.787	228	60
BaS	10.86	2.507	379.4	61	IF	1.948	1.91	610.2	25	RbF	8.5465	2.27	376	60
BF	0.5	1.263	1402.1	62	InCl	3.79	2.401	317.4	25	RbI	11.48	3.177	138.5	57
BH	1.27	1.232	2366.9	63	InF	3.4	1.985	535.4	64	ReN	1.96	0.61		65
BrCl	0.519	2.136	444.3	25	IO	2.45	1.868	681.5	66	RhN	2.43	1.64		67
BrF	1.422	1.759	670.8	25	IrC	1.6	1.683	1060.1	68	RhO	3.81	1.739		69
BrO	1.76	1.717	778.7	41	IrF	2.82	1.851		70	RuF	5.34	1.916		71
CaBr	4.36	2.594	285.3[d]	72	IrN	1.67	1.609		68	ScO	4.55	1.668	965	73
CaCl	4.257	2.439	367.5	72	KBr	10.6281	2.821	213	74	ScS	5.64	2.139	565.2	75
CaD	2.51	2.01		76	KCl	10.2688	2.667	281	60	SD	0.7571	1.341	1885.5	77
CaF	3.07	1.967	581.1	78	KF	8.59255	2.171	428	74	SeF	1.52	1.741	757	66
CaH	2.53	2.003	1298.3	76	KI	10.82	3.048	186.5	57	SeD	0.48	1.47	1708	41
CaI	4.5968	2.829	238.7	79	LaO	3.207	1.826	812.8	52	SeH	0.5	1.47	2400	41
CF	0.65	1.272	1308.1	66	LiBr	7.2262	2.17	563.2	80	SF	0.87	1.596	837.6	66
CH	1.46	1.12	2858.5	25	LiCl	7.1289	2.021	643.3	60	SH	0.758	1.341	2711.6	81
ClD	1.1033	1.275	2145.2	82	LiF	6.32736	1.564	910.3	60	SiH	5.9	1.52	2041.8	41
ClF	0.85	1.628	786.2	83	LiH	5.882	1.596	1405.7	84	SiO	3.0982	1.51	1241.6	85
ClH	1.1085	1.275	2990.9	82	LiI	7.4285	2.392	498.2	86	SiS	1.73	1.73	749.6	87
ClO	1.239	1.57	853.8	88	LiK	3.45	3.27	207	25	SiSe	1.1	2.058	580	37
CN	1.45	1.172	2068.6	89	LiNa	0.47	2.81	256.8	90	SnO	4.32	1.833	814.6	37
CO	0.112	1.128	2169.8	59	LiO	6.84	1.695	851.5	25	SnS	3.18	2.209	487.3	37
CoF	2.82			91	LiRb	4.0	3.466	195.2	25	SnSe	2.82	2.326	331.2	37
CoH	1.88			91	MgD	1.318	1.73	1077.9	92	SnTe	2.19	2.523	259	37
CoO	4.18	1.621		93	MgO	6.2	1.749	785.1	25	SO	1.55	1.481	1149.2	94
CrD	3.51	1.663	1182	95	MoC	6.07			96	SrF	3.4676	2.075	502.4	97
CrN	2.31	1.5652[e]	854.0[f]	98	MoN	3.38	1.63		99	SrO	8.9	1.92	653.5	41
CrO	3.88	1.615	898.4	100	NaBr	9.1183	2.502	302.1	60	ThO	3.534	1.84	895.8	101
CS	1.958	1.535	1285.1	102	NaCl	9.002	2.361	366	60	ThS	4.58	2.35	477[g]	103
CsBr	10.82	3.072	149.7	57	NaCs	4.7	3.851	98.9	41	TiH	2.455			104
CsCl	10.387	2.906	214.2	60	NaF	8.1558	1.926	536	105	TiO	3.34	1.62	1009	106
CSe	1.99	1.676	1035.4	107	NaH	6.4	1.889	1176	108	TiN	3.56	1.582[h]	1039[i]	109
CsF	7.8839	2.345	352.6	60	NaI	9.2357	2.711	258	60	TlBr	4.49	2.618	192.1	41
CsI	11.69	3.315	119.2	57	NaK	2.693	3.589	124.1	25	TlCl	4.5429	2.485	283.8	37
CuF	5.26	1.745	622.7	110	NaRb	3.1	3.644	106.9	25	TlF	4.2282	2.084	477.3	111
CuO	4.57	1.724	640.2	112	NbN	3.26	1.663		113	TlI	4.61	2.814	143	25
CuS	4.31	2.051	415	114	NH	1.39	1.036	3282.3	25	VN	3.07	1.566[j]	1033[k]	98
FeC	2.36	1.61		115	NiH	2.4	1.476	1926.6	116	VO	3.355	1.592[l]	1011.3	117
FeH	2.63			118	NO	0.157	1.151	1904.2	119	VS	5.16	2.06		120
FeO	4.7	1.6	970	121	NS	1.86	1.494	1218.7	66	WC	3.9			122
GaF	2.4	1.774	622.2	41	OD	1.653	0.97	2720.2	41	WN	3.77	1.67[m]		65
GaBr	2.45	2.352	263	37	OF	0.0043	1.354	1028.7	25	YbF	3.91	2.016	501.9	123
GeO	3.2824	1.625	985.5	85	OH	1.6498	0.97	3737.8	124	YF	1.82	1.926	631.3	125
GeS	2	2.012	575.8	37	PbO	4.64	1.922	721	126	YO	4.524	1.79	861	52
GeSe	1.648	2.135	408.7	40	PbS	3.59	2.287	429.4	126	ZrO	2.551	1.712	969.8	52

[a] From ref. 127. [b] From ref. 128. [c] From ref. 129. [d] From ref. 130. [e] From ref. 131. [f] From ref. 132. [g] From ref. 133. [h] From ref. 134. [i] From ref. 135. [j] From ref. 136. [k] From ref. 137. [l] From ref. 138. [m] From ref. 139.

Acknowledgements

We thank Dr Stefan Truppe for reading the manuscript and for useful comments and discussion regarding the nature of the electric dipole moment. Open Access funding provided by the Max Planck Society.

Notes and references

1 A. Kratzer, *Z. Phys.*, 1920, **3**, 289.
2 R. Mecke, *Z. Phys.*, 1925, **32**, 823.
3 P. M. Morse, *Phys. Rev.*, 1929, **34**, 57.
4 R. M. Badger, *J. Chem. Phys.*, 1933, **2**, 128.

5 C. D. Clark and J. L. Stoves, *Nature*, 1934, **133**, 873.
6 C. D. Clark, *London, Edinburgh Dublin Philos. Mag. J. Sci.*, 1934, **18**, 459–470.
7 Y. P. Varshni, *Rev. Mod. Phys.*, 1957, **29**, 664.
8 Y. P. Varshni, *J. Chem. Phys.*, 1958, **28**, 1081.
9 X. Liu, G. Meijer and J. Pérez-Ríos, *On the universality of spectroscopic constants of diatomic molecules*, 2020.
10 S. Hou and P. F. Bernath, *J. Phys. Chem. A*, 2015, **119**, 1435–1438.
11 S. Hou and P. F. Bernath, *Phys. Chem. Chem. Phys.*, 2015, **17**, 4708–4713.
12 G. R. Schleder, A. C. M. Padilha, C. M. Acosta, M. Costa and A. Fazzio, *J. Phys. Mater.*, 2019, **2**, 032001.
13 P. O. Dral, *J. Phys. Chem. Lett.*, 2020, **11**, 2336–2347.
14 F. Noé, A. Tkatchenko, K.-R. Müller and C. Clementi, *Annu. Rev. Phys. Chem.*, 2020, **71**, 361–390.
15 J. Behler, *J. Chem. Phys.*, 2016, **145**, 170901.
16 R. V. Krems, *Phys. Chem. Chem. Phys.*, 2019, **21**, 13392–13410.
17 L. Pauling, *The nature of the chemical bond and the structure of molecules and crystals: an introduction to modern structural chemistry*, Cornell University Press, Ithaca, N.Y., 3rd edn, 1986.
18 R. S. Mulliken, *J. Chem. Phys.*, 1935, **3**, 573–585.
19 C. A. Coulson, *Valence*, Clarendon Press, Oxford, Oxford, United Kingdom, 1952.
20 M. Klessinger, *Angew. Chem., Int. Ed. Engl.*, 1970, **9**, 500–512.
21 C. K. Williams and C. E. Rasmussen, *Gaussian processes for machine learning*, MIT press, Cambridge, MA, 2006, vol. 2.
22 *MATLAB, 9.7.0 (R2019b)*, The MathWorks Inc., Natick, Massachusetts, 2019.
23 S. Raschka, arXiv preprint, 2018, arXiv:1811.12808.
24 X. Liu, G. Meijer and J. Pérez-Ríos, to be published.
25 W. M. Haynes, *CRC handbook of chemistry and physics*, CRC press, 2014.
26 T. Andersen, H. Haugen and H. Hotop, *J. Phys. Chem. Ref. Data*, 1999, **28**, 1511–1533.
27 S. G. Bratsch and J. Lagowski, *Polyhedron*, 1986, **5**, 1763–1770.
28 Atomic Spectra Database - Ionization Energies Form, https://physics.nist.gov/PhysRefData/ASD/ionEnergy.html.
29 J. V. Pototschnig, A. W. Hauser and W. E. Ernst, *Phys. Chem. Chem. Phys.*, 2016, **18**, 5964–5973.
30 N. B. Hannay and C. P. Smyth, *J. Am. Chem. Soc.*, 1946, **68**, 171–173.
31 R. F. Borkman and R. G. Parr, *J. Chem. Phys.*, 1968, **48**, 1116–1126.
32 P. J. Stephens, F. Devlin, C. Chabalowski and M. J. Frisch, *J. Phys. Chem.*, 1994, **98**, 11623–11627.
33 M. Kaupp, P. v. R. Schleyer, H. Stoll and H. Preuss, *J. Chem. Phys.*, 1991, **94**, 1360–1366.
34 T. Leininger, A. Nicklass, W. Küchle, H. Stoll, M. Dolg and A. Bergner, *Chem. Phys. Lett.*, 1996, **255**, 274–280.
35 F. Weigend and R. Ahlrichs, *Phys. Chem. Chem. Phys.*, 2005, **7**, 3297–3305.
36 M. J. Frisch, G. W. Trucks, H. B. Schlegel, G. E. Scuseria, M. A. Robb, J. R. Cheeseman, G. Scalmani, V. Barone, G. A. Petersson, H. Nakatsuji, X. Li, M. Caricato, A. V. Marenich, J. Bloino, B. G. Janesko, R. Gomperts, B. Mennucci, H. P. Hratchian, J. V. Ortiz, A. F. Izmaylov, J. L. Sonnenberg, D. Williams-Young, F. Ding, F. Lipparini, F. Egidi, J. Goings, B. Peng, A. Petrone, T. Henderson, D. Ranasinghe, V. G. Zakrzewski, J. Gao, N. Rega, G. Zheng, W. Liang, M. Hada, M. Ehara, K. Toyota, R. Fukuda, J. Hasegawa, M. Ishida, T. Nakajima, Y. Honda, O. Kitao, H. Nakai, T. Vreven, K. Throssell, J. A. Montgomery, Jr., J. E. Peralta, F. Ogliaro, M. J. Bearpark, J. J. Heyd, E. N. Brothers, K. N. Kudin, V. N. Staroverov, T. A. Keith, R. Kobayashi, J. Normand, K. Raghavachari, A. P. Rendell, J. C. Burant, S. S. Iyengar, J. Tomasi, M. Cossi, J. M. Millam, M. Klene, C. Adamo, R. Cammi, J. W. Ochterski, R. L. Martin, K. Morokuma, O. Farkas, J. B. Foresman and D. J. Fox, *Gaussian 16 Revision C.01*, Gaussian Inc., Wallingford CT, 2016.
37 J. Hoeft, F. Lovas, E. Tiemann and T. Törring, *J. Chem. Phys.*, 1970, **53**, 2736–2743.
38 K. P. Huber and G. Herzberg, *Molecular Spectra and Molecular Structure*, Springer-Verlag, Berlin, Germany, 1979.
39 B. M. Smirnov, *Reference Data on Atomic Physics and Atomic Processes*, Springer-Verlag, Berlin, Germany, 2008.
40 J. Hoeft, F. Lovas, E. Tiemann and T. Törring, *Z. Naturforsch., A: Phys. Sci.*, 1970, **25**, 539.
41 A. A. Radzig and B. M. Smirnov, *Reference data on atoms, molecules, and ions*, Springer Science & Business Media, 2012, vol. 31.
42 J. Hoeft, F. Lovas, E. Tiemann and T. Törring, *Z. Naturforsch., A: Phys. Sci.*, 1970, **25**, 35–39.
43 F. Wyse, E. Manson and W. Gordy, *J. Chem. Phys.*, 1972, **57**, 1106–1108.
44 A. J. Sadlej and M. Urban, *Chem. Phys. Lett.*, 1991, **176**, 293–302.
45 H. Kanata, S. Yamamoto and S. Saito, *J. Mol. Spectrosc.*, 1988, **131**, 89–95.
46 J. Muenter and W. Klemperer, *J. Chem. Phys.*, 1970, **52**, 6033–6037.
47 T. Steimle, K. Jung and B.-Z. Li, *J. Chem. Phys.*, 1995, **103**, 1767–1772.
48 S. Truppe, S. Marx, S. Kray, M. Doppelbauer, S. Hofsäss, H. C. Schewe, N. Walter, J. Pérez-Ríos, B. G. Sartakov and G. Meijer, *Phys. Rev. A*, 2019, **100**, 052513.
49 A. Le, T. C. Steimle, L. Skripnikov and A. V. Titov, *J. Chem. Phys.*, 2013, **138**, 124313.
50 C. Qin, R. Zhang, F. Wang and T. C. Steimle, *J. Chem. Phys.*, 2012, **137**, 054309.
51 T. C. Steimle, R. Zhang, C. Qin and T. D. Varberg, *J. Phys. Chem. A*, 2013, **117**, 11737–11744.
52 R. Suenram, F. Lovas, G. Fraser and K. Matsumura, *J. Chem. Phys.*, 1990, **92**, 4724–4733.
53 K. Jung, T. Steimle, D. Dai and K. Balasubramanian, *J. Chem. Phys.*, 1995, **102**, 643–652.
54 R. Zhang, Y. Yu, T. C. Steimle and L. Cheng, *J. Chem. Phys.*, 2017, **146**, 064307.
55 W. Ernst, J. Kändler and T. Törring, *J. Chem. Phys.*, 1986, **84**, 4769–4773.
56 A. Durand, J. Loison and J. Vigué, *J. Chem. Phys.*, 1997, **106**, 477–484.

57 T. Story Jr and A. Hebert, *J. Chem. Phys.*, 1976, **64**, 855–858.
58 L. Wharton, M. Kaufman and W. Klemperer, *J. Chem. Phys.*, 1962, **37**, 621–626.
59 C. A. Burrus, *J. Chem. Phys.*, 1958, **28**, 427–429.
60 A. Hebert, F. Lovas, C. Melendres, C. Hollowell, T. Story Jr and K. Street Jr, *J. Chem. Phys.*, 1968, **48**, 2824–2825.
61 C. Melendres, A. Hebert and K. Street Jr, *J. Chem. Phys.*, 1969, **51**, 855–856.
62 F. J. Lovas and D. R. Johnson, *J. Chem. Phys.*, 1971, **55**, 41–44.
63 R. Thomson and F. Dalby, *Can. J. Phys.*, 1969, **47**, 1155–1158.
64 J. Hoeft, F. Lovas, E. Tiemann and T. Törring, *Z. Naturforsch., A: Phys. Sci.*, 1970, **25**, 1029–1035.
65 T. C. Steimle and W. L. Virgo, *J. Chem. Phys.*, 2004, **121**, 12411–12420.
66 C. Byfleet, A. Carrington and D. Russell, *Mol. Phys.*, 1971, **20**, 271–277.
67 T. Ma, J. Gengler, Z. Wang, H. Wang and T. C. Steimle, *J. Chem. Phys.*, 2007, **126**, 244312.
68 A. J. Marr, M. Flores and T. Steimle, *J. Chem. Phys.*, 1996, **104**, 8183–8196.
69 J. Gengler, T. Ma, A. G. Adam and T. C. Steimle, *J. Chem. Phys.*, 2007, **126**, 134304.
70 X. Zhuang, T. C. Steimle and C. Linton, *J. Chem. Phys.*, 2010, **133**, 164310.
71 T. C. Steimle, W. L. Virgo and T. Ma, *J. Chem. Phys.*, 2006, **124**, 024309.
72 T. Törring, W. Ernst and S. Kindt, *J. Chem. Phys.*, 1984, **81**, 4614–4619.
73 J. Shirley, C. Scurlock and T. Steimle, *J. Chem. Phys.*, 1990, **93**, 1568–1575.
74 R. Van Wachem, F. De Leeuw and A. Dymanus, *J. Chem. Phys.*, 1967, **47**, 2256–2258.
75 T. Steimle, A. Marr and D. Goodridge, *J. Chem. Phys.*, 1997, **107**, 10406–10414.
76 J. Chen and T. C. Steimle, *J. Chem. Phys.*, 2008, **128**, 144312.
77 W. Meerts and A. Dymanus, *Can. J. Phys.*, 1975, **53**, 2123–2141.
78 W. Childs, L. Goodman, U. Nielsen and V. Pfeufer, *J. Chem. Phys.*, 1984, **80**, 2283–2287.
79 W. Ernst, J. Kändler, J. Lüdtke and T. Törring, *J. Chem. Phys.*, 1985, **83**, 2744–2747.
80 A. Hebert, F. Breivogel Jr and K. Street Jr, *J. Chem. Phys.*, 1964, **41**, 2368–2376.
81 W. Meerts and A. Dymanus, *Astrophys. J.*, 1974, **187**, L45.
82 E. W. Kaiser, *J. Chem. Phys.*, 1970, **53**, 1686–1703.
83 B. Fabricant and J. Muenter, *J. Chem. Phys.*, 1977, **66**, 5274–5277.
84 L. Wharton, L. P. Gold and W. Klemperer, *J. Chem. Phys.*, 1960, **33**, 1255.
85 J. W. Raymonda, J. S. Muenter and W. A. Klemperer, *J. Chem. Phys.*, 1970, **52**, 3458–3461.
86 F. Breivogel Jr, A. Hebert and K. Street Jr, *J. Chem. Phys.*, 1965, **42**, 1555–1558.
87 J. Lovas, F. Hoeft, E. Tiemann and T. Törring, *Z. Naturforsch., A: Phys. Sci.*, 1969, **24**, 1422.
88 T. Amano, S. Saito, E. Hirota, Y. Morino, D. Johnson and F. Powell, *J. Mol. Spectrosc.*, 1969, **30**, 275–289.
89 R. Thomson and F. Dalby, *Can. J. Phys.*, 1968, **46**, 2815–2819.
90 P. Dagdigian, J. Graff and L. Wharton, *J. Chem. Phys.*, 1971, **55**, 4980–4982.
91 H. Wang, X. Zhuang and T. C. Steimle, *J. Chem. Phys.*, 2009, **131**, 114315.
92 T. C. Steimle, R. Zhang and H. Wang, *J. Chem. Phys.*, 2014, **140**, 224308.
93 X. Zhuang and T. C. Steimle, *J. Chem. Phys.*, 2014, **140**, 124301.
94 F. Powell and D. R. Lide Jr, *J. Chem. Phys.*, 1964, **41**, 1413–1419.
95 J. Chen, T. C. Steimle and A. J. Merer, *J. Chem. Phys.*, 2007, **127**, 204307.
96 H. Wang, W. L. Virgo, J. Chen and T. C. Steimle, *J. Chem. Phys.*, 2007, **127**, 124302.
97 W. Ernst, J. Kändler, S. Kindt and T. Törring, *Chem. Phys. Lett.*, 1985, **113**, 351–354.
98 T. C. Steimle, J. S. Robinson and D. Goodridge, *J. Chem. Phys.*, 1999, **110**, 881–889.
99 D. Fletcher, K. Jung and T. Steimle, *J. Chem. Phys.*, 1993, **99**, 901–905.
100 T. C. Steimle, D. F. Nachman, J. E. Shirley, C. W. Bauschlicher Jr and S. R. Langhoff, *J. Chem. Phys.*, 1989, **91**, 2049–2053.
101 F. Wang, A. Le, T. C. Steimle and M. C. Heaven, *Communication: The permanent electric dipole moment of thorium monoxide, ThO*, 2011.
102 G. Winnewisser and R. L. Cook, *J. Mol. Spectrosc.*, 1968, **28**, 266–268.
103 A. Le, M. C. Heaven and T. C. Steimle, *J. Chem. Phys.*, 2014, **140**, 024307.
104 T. Steimle, J. Shirley, B. Simard, M. Vasseur and P. Hackett, *J. Chem. Phys.*, 1991, **95**, 7179–7182.
105 C. Hollowell, A. Hebert and K. Street Jr, *J. Chem. Phys.*, 1964, **41**, 3540–3545.
106 T. C. Steimle and W. Virgo, *Chem. Phys. Lett.*, 2003, **381**, 30–36.
107 J. McGurk, H. Tigelaar, S. Rock, C. Norris and W. Flygare, *J. Chem. Phys.*, 1973, **58**, 1420–1424.
108 P. J. Dagdigian, *J. Chem. Phys.*, 1979, **71**, 2328–2329.
109 B. Simard, H. Niki and P. Hackett, *J. Chem. Phys.*, 1990, **92**, 7012.
110 F. Wang and T. C. Steimle, *J. Chem. Phys.*, 2010, **132**, 054301.
111 R. v. Boeckh, G. Gräff and R. Ley, *Z. Phys.*, 1964, **179**, 285–313.
112 X. Zhuang, S. E. Frey and T. C. Steimle, *J. Chem. Phys.*, 2010, **132**, 234312.
113 D. Fletcher, D. Dai, T. Steimle and K. Balasubramanian, *J. Chem. Phys.*, 1993, **99**, 9324–9325.
114 T. C. Steimle, W.-L. Chang, D. F. Nachman and J. M. Brown, *J. Chem. Phys.*, 1988, **89**, 7172–7179.
115 T. C. Steimle, W. L. Virgo and D. A. Hostutler, *J. Chem. Phys.*, 2002, **117**, 1511–1516.
116 J. A. Gray, S. F. Rice and R. Field, *J. Chem. Phys.*, 1985, **82**, 4717–4718.
117 R. Suenram, G. T. Fraser, F. J. Lovas and C. Gillies, *J. Mol. Spectrosc.*, 1991, **148**, 114–122.

118 T. C. Steimle, J. Chen, J. J. Harrison and J. M. Brown, *J. Chem. Phys.*, 2006, **124**, 184307.
119 A. Hoy, J. Johns and A. McKellar, *Can. J. Phys.*, 1975, **53**, 2029–2039.
120 X. Zhuang and T. C. Steimle, *J. Chem. Phys.*, 2010, **132**, 234304.
121 T. C. Steimle, D. F. Nachman, J. E. Shirley and A. J. Merer, *J. Chem. Phys.*, 1989, **90**, 5360–5363.
122 F. Wang and T. C. Steimle, *Communication: Electric dipole moment and hyperfine interaction of tungsten monocarbide, WC*, 2011.
123 B. Sauer, J. Wang and E. Hinds, *J. Chem. Phys.*, 1996, **105**, 7412–7420.
124 D. D. Nelson Jr, A. Schiffman and D. J. Nesbitt, *J. Chem. Phys.*, 1989, **90**, 5455–5465.
125 J. Shirley, C. Scurlock, T. Steimle, B. Simard, M. Vasseur and P. Hackett, *J. Chem. Phys.*, 1990, **93**, 8580–8585.
126 J. Hoeft, F. Lovas, E. Tiemann, R. Tischer and T. Törring, *Z. Naturforsch., A: Phys. Sci.*, 1969, **24**, 1222–1226.
127 P. Schwerdtfeger, J. S. McFeaters, M. J. Liddell, J. Hrušák and H. Schwarz, *J. Chem. Phys.*, 1995, **103**, 245–252.
128 T. Okabayashi, F. Koto, K. Tsukamoto, E. Yamazaki and M. Tanimoto, *Chem. Phys. Lett.*, 2005, **403**, 223–227.
129 A. J. Parsons, S. P. Gleason and T. D. Varberg, *Mol. Phys.*, 2018, **116**, 3547–3553.
130 P. Bernath, R. Field, B. Pinchemel, Y. Lefebvre and J. Schamps, *J. Mol. Spectrosc.*, 1981, **88**, 175–193.
131 P. Sheridan, M. Brewster and L. M. Ziurys, *Astrophys. J.*, 2002, **576**, 1108.
132 J. F. Harrison, *J. Phys. Chem.*, 1996, **100**, 3513–3519.
133 J. H. Bartlett, I. O. Antonov and M. C. Heaven, *J. Phys. Chem. A*, 2013, **117**, 12042–12048.
134 T. Dunn, L. K. Hanson and K. A. Rubinson, *Can. J. Phys.*, 1970, **48**, 1657–1663.
135 A. Douglas and P. Veillette, *J. Chem. Phys.*, 1980, **72**, 5378–5380.
136 W. J. Balfour, A. J. Merer, H. Niki, B. Simard and P. A. Hackett, *J. Chem. Phys.*, 1993, **99**, 3288–3303.
137 B. Simard, C. Masoni and P. Hackett, *J. Mol. Spectrosc.*, 1989, **136**, 44–55.
138 A. J. Merer, *Annu. Rev. Phys. Chem.*, 1989, **40**, 407–438.
139 R. Ram and P. Bernath, *J. Opt. Soc. Am. B*, 1994, **11**, 225–230.